



## Ultrafine Particulate Matter Source Contributions across the Continental United States

Melissa A. Venecek<sup>a</sup>, Xin Yu<sup>b</sup> and Michael J. Kleeman<sup>b</sup>

5

<sup>a</sup>Department of Land, Air and Water Resources, University of California Davis, Davis, CA

<sup>b</sup>Department of Civil and Environmental Engineering, University of California Davis, Davis, CA

10 \*Corresponding author. Tel.: +1 530 752 8386; fax; +1 530 752 7872. E-mail address:  
mjkleeman@ucdavis.edu (M.J. Kleeman).



## Abstract

The regional concentration of airborne ultrafine particulate matter mass ( $D_p < 0.1 \mu\text{m}$ ;  $\text{PM}_{0.1}$ ) was predicted with 4 km resolution in 39 cities across the United States during summer time air pollution episodes. Calculations were performed using a regional chemical transport model with 4 km spatial resolution operating on the National Emissions Inventory created by the US EPA. Measured source profiles for particle size and composition between  $0.01 - 10 \mu\text{m}$  were used to translate PM total mass to  $\text{PM}_{0.1}$ .  $\text{PM}_{0.1}$  concentrations exceeded  $2 \mu\text{g m}^{-3}$  during summer pollution episodes in major urban regions across the US including Los Angeles, the San Francisco Bay Area, Houston, Miami, and New York.  $\text{PM}_{0.1}$  spatial gradients were sharper than  $\text{PM}_{2.5}$  spatial gradients due to the dominance of primary aerosol in  $\text{PM}_{0.1}$ . Artificial source tags were used to track contributions to primary  $\text{PM}_{0.1}$  and  $\text{PM}_{2.5}$  from fifteen source categories. As expected, on-road gasoline and diesel vehicles made significant contributions to regional  $\text{PM}_{0.1}$  in all 39 cities even though peak contributions within 0.3 km of the roadway were not resolved by the 4 km grid cells. Food cooking also made significant contributions to  $\text{PM}_{0.1}$  in all cities but biomass combustion was only important in locations impacted by summer wildfires. Aviation was a significant source of  $\text{PM}_{0.1}$  in cities that had airports within their urban footprints. Industrial sources including cement manufacturing, process heating, steel foundries, and paper & pulp processing impacted their immediate vicinity but did not significantly contribute to  $\text{PM}_{0.1}$  concentrations in any of the target 39 cities. Natural gas combustion made significant contributions to  $\text{PM}_{0.1}$  concentrations due to the widespread use of this fuel for electricity generation, industrial applications, residential, and commercial use. The major sources of primary  $\text{PM}_{0.1}$  and  $\text{PM}_{2.5}$  were notably different in many cities. Future epidemiological studies may be able to differentiate  $\text{PM}_{0.1}$  and  $\text{PM}_{2.5}$  health effects by contrasting cities with different ratios of  $\text{PM}_{0.1} / \text{PM}_{2.5}$ . In the current study, cities with higher  $\text{PM}_{0.1} / \text{PM}_{2.5}$  ratios include Houston TX, Los Angeles CA, Birmingham AL, Charlotte NC, and Bakersfield CA. Cities with lower  $\text{PM}_{0.1}$  to  $\text{PM}_{2.5}$  ratios include Lake Charles LA, Baton Rouge LA, St. Louis MO, Baltimore MD, and Washington DC.



## 1. Introduction

Airborne particulate matter (PM) has been linked with premature mortality and numerous other health risks in cities across the world (see for example references (Laden, Neas et al. 2000, Pope, Burnett et al. 2002, Dominici, Peng et al. 2006, Ostro, Broadwin et al. 2006, Franklin, Zeka et al. 2007, Pope, Ezzati et al. 2009, Kheirbek, Wheeler et al. 2013, Aneja, Pillai et al. 2017)). Despite years of progress (EPA 2017), PM concentrations in many urban regions in the United States still exceed health-based standards resulting in an increase of non-accidental mortality (Franklin, Zeka et al. 2007, Baxter, Duvall et al. 2013). Toxicology testing suggests that ultrafine particles with diameter  $< 0.1 \mu\text{m}$  may be the most harmful size fraction within  $\text{PM}_{2.5}$  (Oberdorster, Gelein et al. 1995, Pekkanen, Timonen et al. 1997, Oberdorster 2000, Li, Siotas et al. 2003, Ostro, Hu et al. 2015). Initial attempts to analyze ultrafine particles in epidemiology studies have used particle number concentration as a surrogate for ultrafine particle exposure, but this approach has not found consistent relationships with health effects (Ostro, Hu et al. 2015). In contrast, a recent epidemiology study based on ultrafine particle mass ( $\text{PM}_{0.1}$ ) found significant associations with premature mortality (Ostro, Hu et al. 2015). Follow-up studies have also found significant associations between  $\text{PM}_{0.1}$  and reproductive outcomes including birth weight and preterm birth (Bergin, Russell et al. 1996, Laurent, Hu et al. 2016). These findings have biological plausibility, since ultrafine particles may cross cell membranes and interfere with the internal cell function (Siotas, Delfino et al. 2005). The toxic material found in ultrafine particles has greater surface area due to the small particle diameter making the material more available for chemical reaction. Ultrafine particles can therefore have a larger impact when deposited deep into the lung cavity where they are not easily removed (Li, Siotas et al. 2003, Nel, Xia et al. 2006).

A national monitoring network for  $\text{PM}_{10}$  and  $\text{PM}_{2.5}$  has been operating throughout the continental US for almost 20 years. Multiple studies have performed source apportionment calculations for coarse and fine PM using these measurements (Zheng, Cass et al. 2002, Reff, Bhawe et al. 2009, Ham and Kleeman 2011, Zhang, Hu et al. 2014). In contrast, measurements of  $\text{PM}_{0.1}$  are limited to focused field campaigns lasting for short time periods with even fewer studies attempting source apportionment calculations (Kleeman, Riddle et al. 2009). Multiple barriers have prevented the widespread deployment of  $\text{PM}_{0.1}$  monitoring networks including (i) the low concentration of  $\text{PM}_{0.1}$  mass, which challenges the detection limits of analytical methods,



(ii) the artifacts associated with collecting  $PM_{0.1}$  samples, (iii) the additional workload involved in operating the collection devices, and (iv) the sharp spatial gradients of  $PM_{0.1}$  fields.

Expensive investments in  $PM_{0.1}$  monitoring are unlikely to occur without compelling evidence  
75 linking  $PM_{0.1}$  to public health. Early epidemiological studies for  $PM_{0.1}$  must therefore use some other technique besides direct measurements to calculate population exposure.

Various methods such as the source-resolved PMCAMx chemical transport model, the chemical mass balance (CMB) model, photochemical box models and land use regression (LUR) models have been used to track source contributions to primary organic matter, elemental carbon  
80 and in some cases particle number concentration (PNC) over areas in the Eastern U.S. and parts of Europe and Asia (Gaydos, Stanier et al. 2005, Lane, Pinder et al. 2007, Wang, Hopke et al. 2011, Posner and Pandis 2015, Cattani, Gaeta et al. 2017, Wolf, Cyrus et al. 2017, Simon, Patton et al. 2018, Zhong, Nikolova et al. 2018). However, these methods are limited in one or more aspects of their ability to predict population exposure ultrafine particles over large analysis  
85 domains. Source resolved models, such as PMCAMx, have been demonstrated for PNC but not for  $PM_{0.1}$  (Posner and Pandis 2015). CMB models need measurements of specific molecular markers at numerous sites to resolve the sharp spatial gradients of ultrafine particle source contributions. LUR models need comprehensive measurements that act as training data sets in order to extend throughout a modeling domain (Lane, Pinder et al. 2007).

90 Hu et al. (Hu, Zhang et al. 2014) calculated population exposure to  $PM_{0.1}$  in California using a regional source-oriented chemical transport model supported by measured profiles for particle size and composition emitted by dominant sources. Predictions were compared to all available fine and ultrafine particle measurements over the period 2000-2010 with good agreement observed for the dominant chemical components of  $PM_{0.1}$  mass including organic  
95 aerosol, elemental carbon, and numerous trace metals (Hu, Zhang et al. 2014). The 4km spatial resolution used in these calculations supported multiple epidemiological studies based on spatial gradients of exposure (Ostro, Hu et al. 2015, Laurent, Hu et al. 2016). These encouraging results motivate the expansion of the  $PM_{0.1}$  exposure technique to other locations.

Here we use the Eulerian source-oriented UCD/CIT chemical transport model to predict  
100 the concentration of  $PM_{0.1}$  in thirty-nine urban regions throughout the US during summer pollution events in 2010. The calculation tracks contributions from fifteen (15) primary particle sources through a simulation of all major atmospheric processes while retaining information



about particle size, composition and source origin (Hu, Zhang et al. 2014). The results of this calculation reveal US national trends in  $PM_{0.1}$  concentrations for the first time and suggest  
 105 locations where the differential health effects of  $PM_{0.1}$  and  $PM_{2.5}$  can best be studied.

## 2. Methods

### 2.1 Simulation Dates

Simulations within each target city were carried out during peak summer air pollution  
 110 events in 2010. Peak air pollution events typically had measured 1-hr maximum ozone ( $O_3$ ) concentrations greater than 70 ppb. Regional pollution events caused by atmospheric stagnation were selected whenever possible as opposed to special events caused by unusual occurrences such as wildfires. Measured  $PM_{2.5}$  24-hr concentrations during peak summer pollution events ranged between 3.2–30  $\mu g/m^3$  depending on the location. The simulation dates in each city are  
 115 listed in Table 1 and a map of the city locations is shown in the supplemental information Figure S1. The aggregation of these events across the US enables a comparison of typical air pollution episodes within different cities.

Table 1. City, Simulation Date, 2010 Population and Geographical Region

City	2010 Date	2010 Population	US Geographical Region
Atlanta	March 29 - April 1	422765	South East
Austin	August 23 - August 26	815260	South
Bakersfield	August 23 - August 26	348938	West
Baltimore	August 7 - August 10	621210	East Coast
Baton Rouge	October 6 - October 9	229584	South
Birmingham	October 6 - October 9	212107	South East
Boston	August 29 - September 1	620451	East Coast
Charlotte	March 30 - April 2	738710	South East
Cincinnati	August 25 - August 28	296904	Midwest
Cleveland	August 25 - August 28	396009	Midwest
Dallas	August 23 - August 26	1201000	South
Denver	July 13 - July 16	603421	West
Detroit	August 25 - August 28	711299	Midwest
El Paso	July 11 - July 14	651665	West
Fresno	August 23 - August 26	497090	West



City	2010 Date	2010 Population	US Geographical Region
Hartford	August 29 - September 1	125312	East Coast
Houston	October 6 - October 9	2103000	South
Indianapolis	August 25 - August 28	830952	Midwest
Jacksonville	March 29 - April 1	823291	South East
Kansas City	August 25 - August 28	460639	Midwest
Lake Charles	October 6 - October 9	72268	South
Los Angeles	September 23 - September 26	3796000	West
Louisville	August 7 - August 10	300000	Midwest
Memphis	October 6 - October 9	647609	Midwest
Miami	March 30 - April 2	400769	South East
Nashville	October 7 - October 10	1800000	Midwest
New York City	August 29 - September 1	8190000	East Coast
Philadelphia	August 27 - August 30	1529000	East Coast
Phoenix	June 19 - Jun3 22	1449000	West
Portland	August 23 - August 26	585286	West
Richmond	August 7 - August 10	204351	East Coast
Sacramento	August 22 - August 25	466488	West
Salt Lake City	August 18 - August 21	186505	West
San Antonio	August 23 - August 26	1334000	South
San Diego	September 23 - September 26	1306000	West
San Francisco	August 22 - August 25	805704	West
St. Louis	August 25 - August 28	319257	Midwest
Tulsa	August 25 - August 28	392443	Midwest
Washington DC	August 7 - August 10	604453	East Coast

120

## 2.2 Model Description

The UCD/CIT model predicts the evolution of gas and particle phase pollutants in the atmosphere in the presence of emissions, transport, deposition, chemical reaction and phase change (Held, Ying et al. 2005) as represented by Eq. (1)

125

$$\frac{\partial C_i}{\partial t} + \nabla \cdot u C_i = \nabla K \nabla C_i + E_i - S_i + R_i^{gas}(C) + R_i^{part}(C) + R_i^{phase}(C) \quad (1)$$



where  $C_i$  is the concentration of gas or particle phase species  $i$  at a particular location as a  
 130 function of time  $t$ ,  $u$  is the wind vector,  $K$  is the turbulent eddy diffusivity,  $E_i$  is the emissions  
 rate,  $S_i$  is the loss rate,  $R_i^{gas}$  is the change in concentration due to gas-phase reactions,  $R_i^{part}$  is the  
 change in concentration due to particle-phase reactions and  $R_i^{phase}$  is the change in concentration  
 due to phase change (Held, Ying et al. 2005). Loss rates include both dry and wet deposition.  
 Phase change for inorganic species occurs using a kinetic treatment for gas-particle conversion  
 135 (Hu, Zhang et al. 2008) driven towards the point of thermodynamic equilibrium (Nenes, Pilinis  
 et al. 1998). Phase change for organic species is also treated as a kinetic process with vapor  
 pressures of semi-volatile organics calculated using the 2-product model (Carlton, Bhawe et al.  
 2010). More sophisticated approaches for secondary organic aerosol (SOA) formation (Cappa,  
 Jathar et al. 2016) were also tested in the current study but these required a larger number of  
 140 assumptions and they did not produce higher SOA concentrations in the  $PM_{0.1}$  size fraction.  
 Nucleation was not included in the current study and so particle number concentrations will not  
 be discussed. Likewise, model spatial resolution was 4km over the 4.2 million  $km^2$  of simulated  
 urban areas and so near-roadway concentrations of ultrafine particles on spatial scales of  $\sim 0.1$  km  
 will not be presented.

145 A total of 50 particle-phase chemical species are included in each of 15 discrete particle  
 size bins that range from 0.01-10  $\mu m$  particle diameter (Held, Ying et al. 2005). Artificial source  
 tags are used to quantify source contributions to the primary particle mass for a specific bin size,  
 therefore allowing for the direct contribution of each source of  $PM_{2.5}$  and  $PM_{0.1}$  mass to be  
 determined. Gas-phase concentrations of oxides of nitrogen ( $NO_x$ ), volatile organic compounds  
 150 (VOCs), oxidants, ozone, and semi-volatile reaction products were predicted using the SAPRC-  
 11 chemical mechanism (Carter and Heo 2013).

### 2.3 Model Inputs

Anthropogenic emissions were generated using the Sparse Matrix Operator Kernel  
 155 Emissions (SMOKEv3.7) modeling system applied to the 2011 National Emissions Inventory.  
 Emissions from each of the four major source sectors (area, mobile, non-road and point) were  
 tagged to create fifteen (15) different emissions groups: on road diesel, on road gasoline, off road  
 diesel, off road gasoline, biomass, food cooking, natural gas, process heaters, distillate oil,  
 aviation, cement, coal, steel foundries, paper products and all other emissions. Size and



160 composition-resolved source profiles were then assigned to the PM emissions within each of  
these groups using the UCD/CIT emissions processor based on the most recent measurements  
available in the literature (Robert, VanBergen et al. 2007a, Robert, Kleeman et al. 2007b,  
Kleeman, Robert et al. 2008). Some of the fifteen (15) source categories were represented using  
weighted average source profiles from multiple sources as described in Table S1.

165 Daily values for 2010 wildfire emissions were generated using the Global Fire Emissions  
Database (GFED) (Giglio, Randerson et al. 2013). Biogenic emission rates were generated using  
the Model of Emissions of Gases and Aerosols from Nature (MEGANv2.1). The gridded geo-  
referenced emission factors and land cover variables required for MEGAN calculations were  
created using the MEGANv2.1 pre-processor tool and the ESRI\_GRID leaf area index and plant  
170 functional type files available at the Community Data Portal (Guenther, Jiang et al. 2012).

Meteorology parameters used to drive the UCD/CIT CTM were generated using the  
Weather Research and Forecasting model (WRFv3.6) and WRF preprocessing system  
(WPSv3.6). Meteorological fields were created within 3 nested domains with horizontal  
resolutions of 36km, 12km, and 4km, respectively. Each domain had 31 telescoping vertical  
175 levels up to a top height of 12km. Four-dimensional data assimilation (FDDA) or “FDDA  
nudging” was used to anchor meteorological predictions to measured values (Hu et al., 2010).  
Meteorological data and gridded map projections needed for 2010 emissions modeling were  
taken from the corresponding WRF simulations using the meteorology-chemistry interface  
processor (MCIP).

180

### 2.3 Supporting Measurements

Ambient hourly ozone measurements and daily PM<sub>2.5</sub> measurements were obtained from  
the EPA AQS API / Query AirData (EPA). Model predictions are compared to these  
measurements to build confidence in the accuracy of the overall modeling system since PM<sub>0.1</sub>  
185 measurements are not available during any of the peak summer pollution events studied here.

### 3. Results

Predicted 1-hr ozone concentrations were compared to measurements averaged within  
each city to indirectly evaluate the accuracy of the emissions inventories and meteorology fields.  
190 Many of the sources that emit ozone precursors also emit ultrafine particles. Likewise,





meteorological parameters including wind speed and mixing depth influence the concentrations of all pollutants including ultrafine particles. Successful prediction of ozone is therefore a necessary step in the accurate prediction of ultrafine particle concentrations during summer photochemical smog episodes. Figure 1 illustrates the time series of predicted vs measured  
 195 ozone concentration for four (4) representative cities spanning the South, East, Midwest and West US regions. The full set of comparisons for all 39 cities are shown in the supplemental information Figure S2. In general, model simulations capture the peak ozone concentration and diurnal pattern during the pollution events. Mean fractional bias (MFB) and mean fractional error (MFE) summary statistics meet EPA criteria in 37 out of 39 cities (Table S2 in the supplemental  
 200 information).

Predicted 24-hr  $PM_{2.5}$  concentrations were compared to measurements as a second check on the accuracy of model features needed to predict ultrafine particle concentrations. Many of the combustion sources that emit primary particles within the  $PM_{2.5}$  size fraction also emit  $PM_{0.1}$ . The Chemical Speciation Monitoring Network (CSN) operated by the U.S. Environmental  
 205 Protection Agency (EPA) measures  $PM_{2.5}$  mass and chemical composition at more than 260 sites throughout the U.S. including many of the 39 cities studied in the current analysis (Solomon, Crumpler et al. 2014). Elemental carbon (EC) and organic compounds (OC) are the chemical components most relevant for both the  $PM_{2.5}$  and the  $PM_{0.1}$  size fractions. Figure 2 illustrates predicted vs measured 24-hr  $PM_{2.5}$  EC and OC concentrations for all 39 cities while Figure S3  
 210 illustrates predicted vs. measured 24-hr  $PM_{2.5}$  total mass comparisons. In general, the model slightly under predicts  $PM_{2.5}$  EC, OC, and mass with regression slopes ranging from 0.62 for EC to 0.97 for OC. The negative bias in model predictions may stem from the 4km spatial averaging inherent in the calculations vs. the influence of sources closer than 4 km to the measurement site in the urban environment such as highways, restaurants, etc. This trend is reflected in the  
 215 performance of ozone predictions during the evening hours for Los Angeles and New York City (Figure 1), where measured ozone concentrations fall to zero due to titration from nearby  $NO_x$  emissions while predicted ozone concentrations remain greater than zero due to dilution of  $NO_x$  emissions within 4 km grid cells. The MFB and MFE for  $PM_{2.5}$  predictions are summarized in the supplemental information Table S2.

220 As was the case for ozone predictions,  $PM_{2.5}$  model performance meets EPA criteria (MFE<0.75) in 37 out of 39 cities, building confidence in the accuracy of the model results for



PM concentrations. MFB values lower than 0.15 and MFE values lower than 0.35 are considered the goal or “excellent” in model performance. In the current study, the average MFB and MFE across all 39 cities was 0.126 and 0.379 for  $O_3$ , and -0.27 and 0.38 for  $PM_{2.5}$  respectively.

225  $PM_{0.1}$  measurements are not available for model evaluation in the 39 cities across the US in 2010 at the core of the current study, but measurements are available in California in the years 2015 and 2016 that can serve to evaluate similar modeling procedures. Yu et al. (Yu, Venecek et al. 2018) compared  $PM_{0.1}$  concentrations in Los Angeles, Fresno, East Oakland, and San Pablo, California predicted using the UCD/CIT air quality model to receptor-based source  
 230 apportionment calculations based on measured concentrations of molecular markers in the ultrafine particle size fraction (Xue, Xue et al. 2018). Good agreement was found between predictions from these two independent techniques for  $PM_{0.1}$  concentrations associated with gasoline engines, diesel engines, food cooking, wood burning, and “other sources”. Further details of this comparison are provided by (Yu, Venecek et al. 2018). This evaluation of the  
 235 modeling procedures builds confidence in the  $PM_{0.1}$  source predictions across the US in the current study.

Figure 3 illustrates a composite representation of  $PM_{2.5}$  and  $PM_{0.1}$  mass across the US during the summer pollution episodes listed in Table 1. The spatial plot in Figure 3 is constructed using the intermediate 12km simulation results from multiple simulations stitched  
 240 together to cover a broader geographical area. Regional  $PM_{0.1}$  concentrations reach a maximum value of  $5 \mu g m^{-3}$  in a few isolated grid cells with wildfires but concentrations generally exceed  $2 \mu g m^{-3}$  in major urban regions across the US including Los Angeles, the San Francisco Bay Area, Houston, Miami, and New York. The comparison between  $PM_{2.5}$  mass (Figure 3a) and  $PM_{0.1}$  mass (Figure 3b) shows that  $PM_{0.1}$  spatial gradients are sharper with less regional contributions  
 245 between “hot spots”. Locations in the Midwestern and Eastern US outside of cities with high  $PM_{2.5}$  concentrations due to secondary formation (sulfate and secondary organic aerosol) did not have corresponding high concentrations of  $PM_{0.1}$ . Most major urban centers had noticeable peaks of both  $PM_{2.5}$  and  $PM_{0.1}$ . This pattern presents a challenge for epidemiological studies seeking to differentiate the effects of  $PM_{2.5}$  and  $PM_{0.1}$  because the locations with differential  
 250 exposure (high  $PM_{2.5}$  but low  $PM_{0.1}$ ) have low population density which will reduce the power of the analysis.



The UCD/CIT model explicitly tracks source contributions to particle mass in each size bin using artificial source tags. Pie charts of  $PM_{2.5}$  and  $PM_{0.1}$  source contributions are illustrated in Figure 3 for selected major cities. Pie charts for  $PM_{0.1}$  source contributions in all 39 US cities are shown in Figure 4. The detailed source profiles within each city are based on the nested 4km simulation results during the pollution events listed in Table 1. Source contribution spatial plots for the entire US are shown in the supplemental information Figures S4-S7 and pie charts for  $PM_{2.5}$  source contributions in all 39 US cities are shown in the supplemental information Figure S8. As expected, on-road gasoline and diesel vehicles made significant contributions to regional  $PM_{0.1}$  in all 39 cities even though peak contributions within 0.3 km of the roadway were not resolved by the 4 km grid cells. Food cooking also made significant contributions to  $PM_{0.1}$  in all cities but biomass combustion was only important in locations impacted by summer wildfires. Aviation was a significant source of  $PM_{0.1}$  in cities that had airports within their urban footprints. Industrial sources including cement manufacturing, process heating, steel foundries, and paper & pulp processing impacted their immediate vicinity but did not significantly contribute to  $PM_{0.1}$  concentrations in any of the target 39 cities. Natural gas combustion made significant contributions to  $PM_{0.1}$  concentrations due to the widespread use of this fuel for residential, commercial, and industrial applications. Natural gas contributions were especially significant in locations with high levels of industrial use such as chemical refineries or in locations with significant levels of natural gas fired power plants.

The major sources of primary  $PM_{0.1}$  and  $PM_{2.5}$  were notably different in many cities (compare Figure 3a and 3b). The sources that contribute most strongly to  $PM_{2.5}$  are on road diesel, gasoline, food cooking, coal and “other” which includes break and tire wear from mobile sources and dust. Natural gas combustion makes minor contributions to primary  $PM_{2.5}$  mass since particles from this source have a mass distribution peaking at  $\sim 0.05 \mu m$  particle diameter (Chang, Chow et al. 2004) with all of the emitted mass in the  $PM_{0.1}$  size fraction. In contrast, other combustion sources using more complex fuels such as on-road vehicles have a mass distribution peaking at  $\sim 0.1 \mu m$  with at least half the emitted mass outside the  $PM_{0.1}$  size fraction (Robert, VanBergen et al. 2007a, Robert, Kleeman et al. 2007b). Likewise, food cooking contributes strongly to  $PM_{2.5}$  concentrations but the emitted particle mass distribution peaks at  $0.2 \mu m$  with the majority of the mass outside the  $PM_{0.1}$  size fraction.

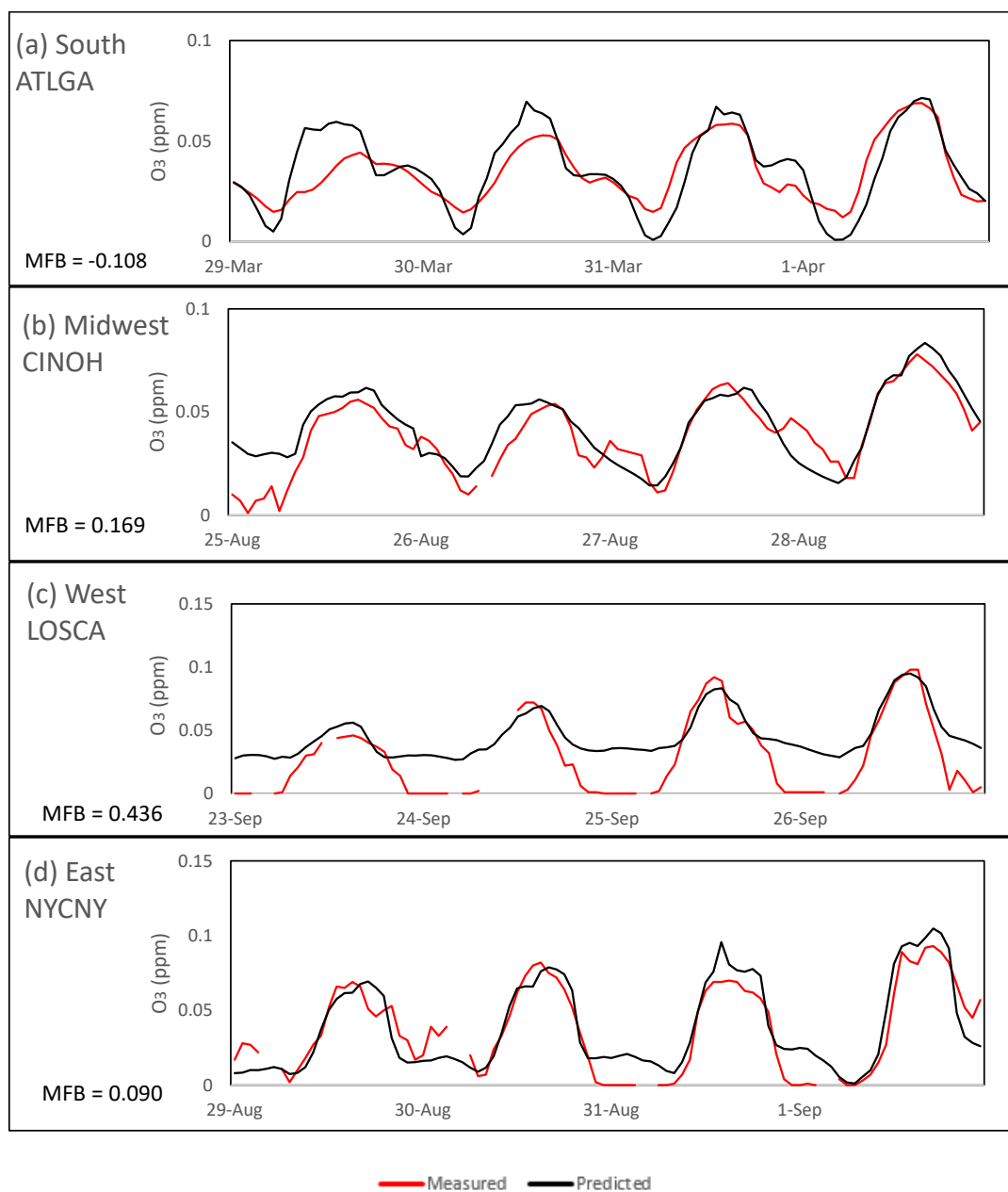


Figure 1. Time series of 1-hr measured vs predicted ozone concentration (ppm) for 4 selected city scenarios representative of the major geographical regions across the Continental United States

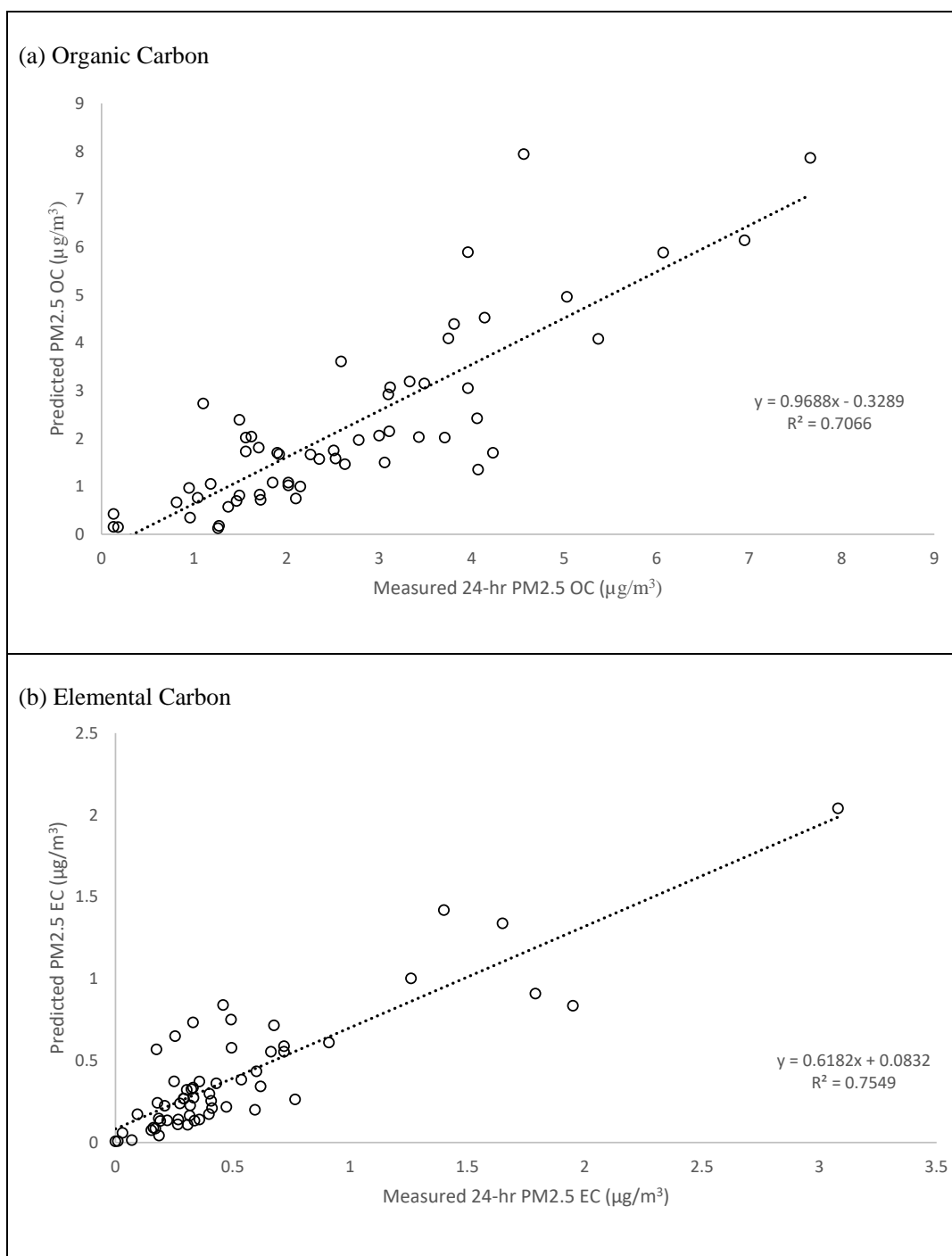
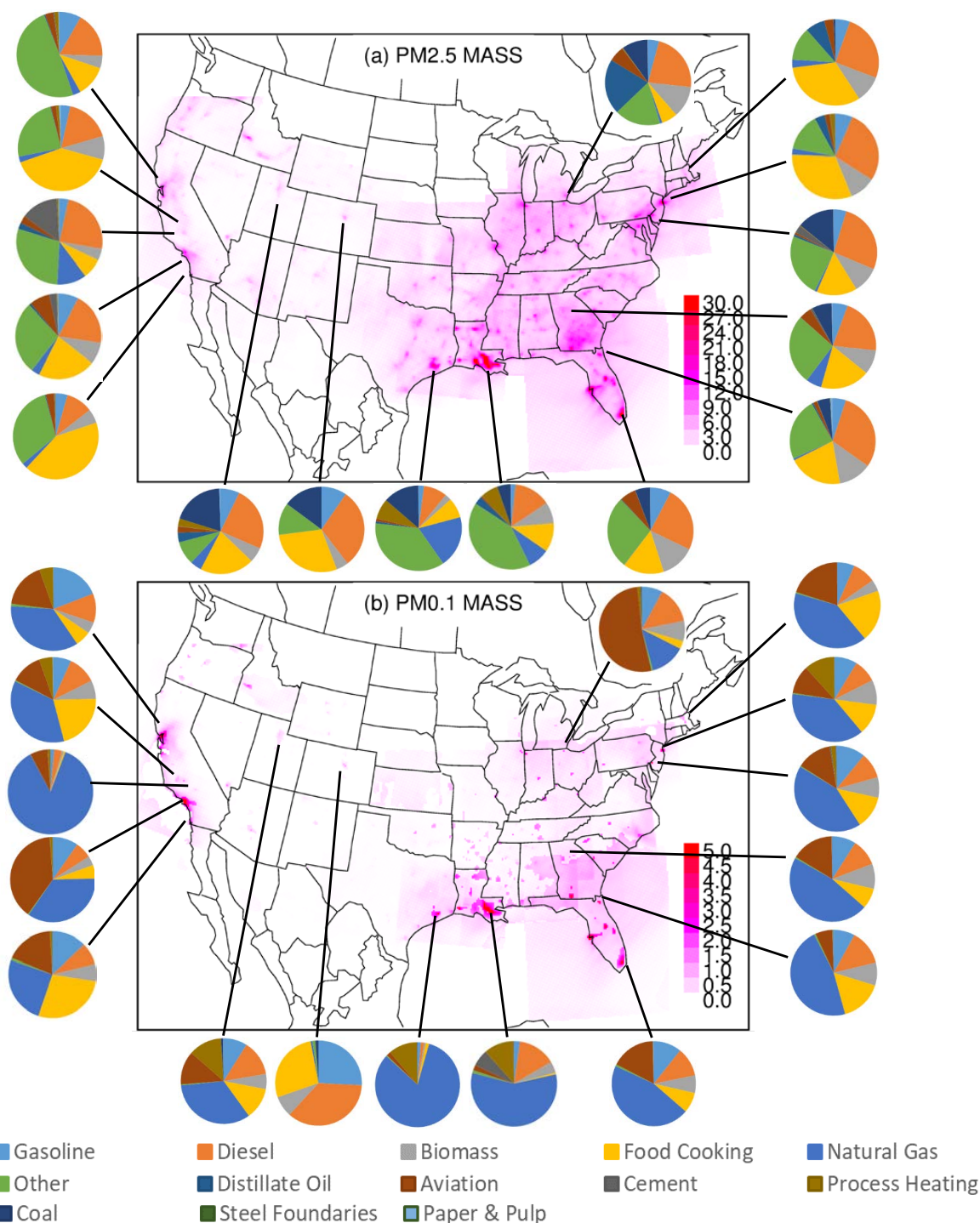


Figure 2. Predicted vs Measured (a) Organic Carbon and (b) Elemental Carbon ( $\mu\text{g m}^{-3}$ )



295

300 Figure 3. (a) PM<sub>2.5</sub> and (b) PM<sub>0.1</sub> 24-hr average mass ( $\mu\text{g m}^{-3}$ ) during summer air pollution event. Scale drawn to highlight all areas of US. Actual Max for (a) = 109.28  $\mu\text{g m}^{-3}$  (b) = 7.71  $\mu\text{g m}^{-3}$ .

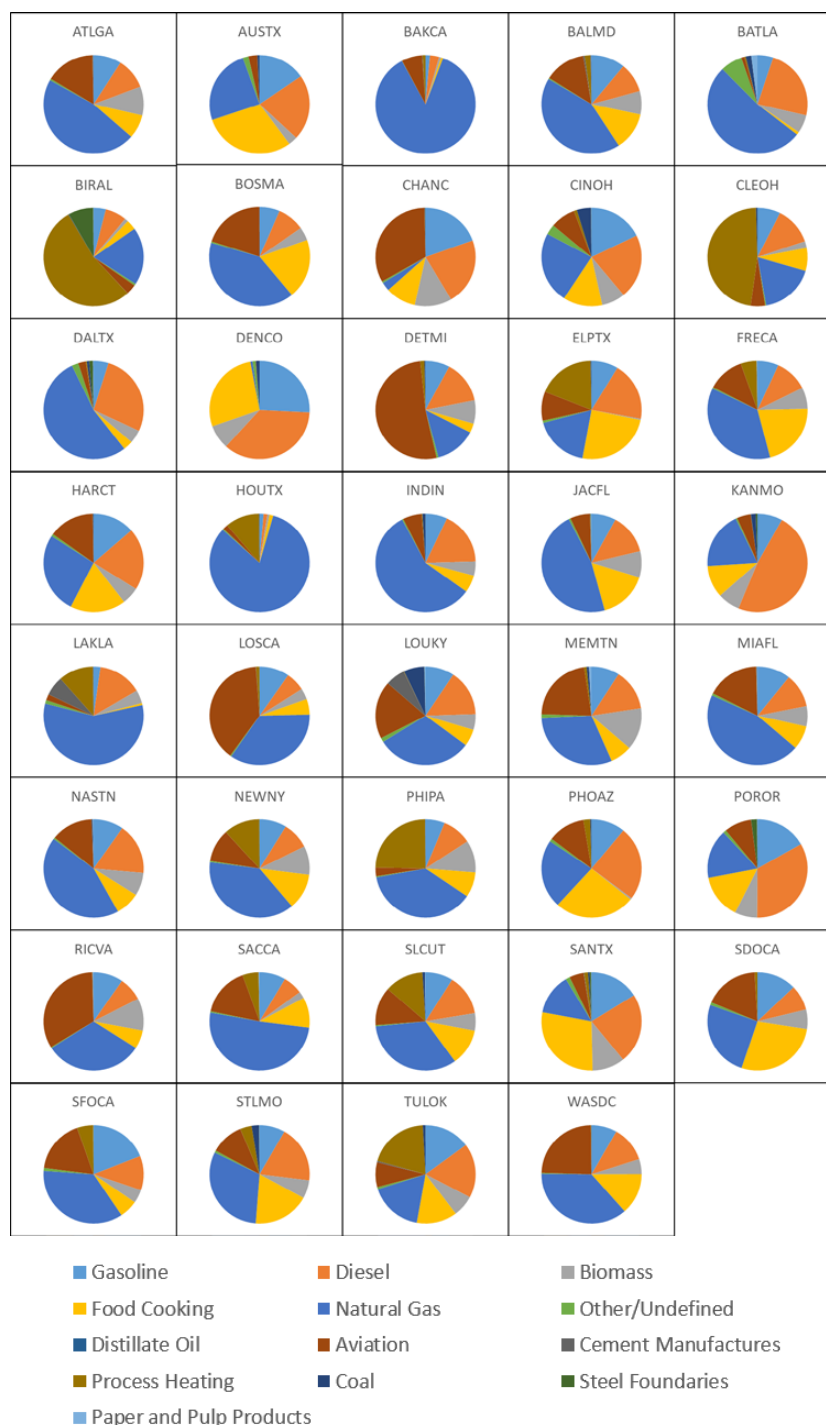


Figure 4.  $PM_{0.1}$  source contribution for 39 cities across the continental US





305

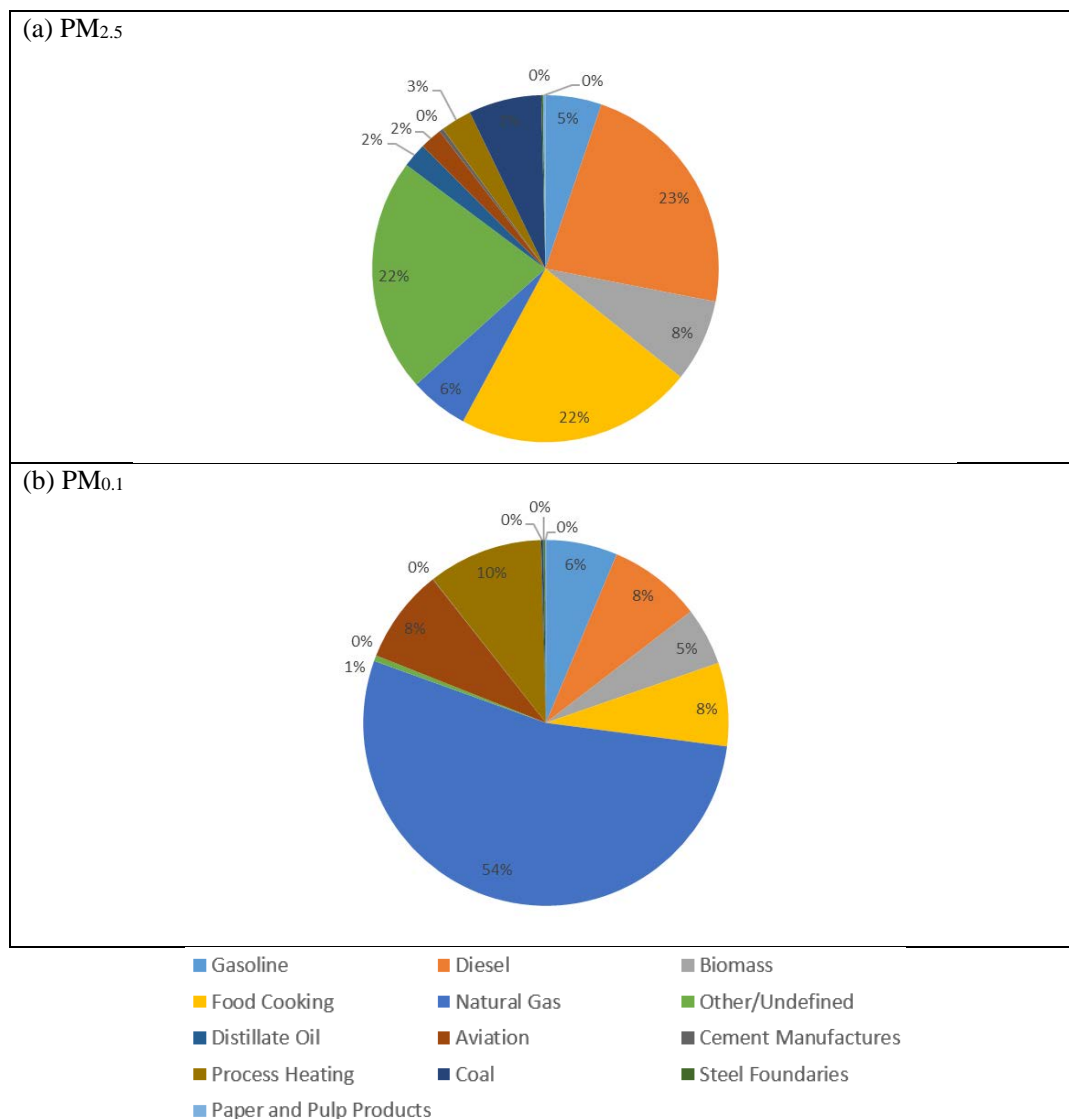


Figure 5. Population weighted average source contribution across the 39 major cities in the continental US for (a) PM<sub>2.5</sub> and (b) PM<sub>0.1</sub>





#### 310 4. Discussion

Figure 5 illustrates the population-weighted average  $PM_{0.1}$  source contributions across all 39 study cities shown in Table 1. This calculation highlights the importance of natural gas combustion particles in the  $PM_{0.1}$  size fraction and the minor role that these natural gas combustion particles play in the  $PM_{2.5}$  size fraction. Natural gas typically consists of +93% methane with the balance of the fuel made up by higher molecular weight alkanes and trace impurities. In addition to background sulfur compounds in the natural gas, sulfur-containing odorants such as mercaptans are commonly added to aid in leak detection.

Natural gas combustion does not emit high amounts of particulate matter per J of energy in the fuel, but the widespread use of natural gas suggests that it could still contribute significantly to ambient  $PM_{0.1}$  concentrations. Natural gas combustion accounted for 29% of total US energy consumption in 2016 (Energy 2017). In contrast, gasoline combustion accounted for 17% of US energy consumption and diesel fuel combustion accounted for approximately 6% of US energy consumption in 2016. Gasoline and diesel fuel combustion in motor vehicles also emit most particles in the size fraction larger than  $PM_{0.1}$  (Robert, VanBergen et al. 2007a, Robert, Kleeman et al. 2007b) whereas natural gas combustion emits particles entirely within the  $PM_{0.1}$  size fraction (Chang, Chow et al. 2004). Taken together, these facts support the potential importance of natural gas combustion for ambient  $PM_{0.1}$  concentrations.

The five (5) states with the highest consumption of natural gas in 2016 were Texas (14.7%), California (7.9%), Louisiana (5.7%), New York (5%), and Florida (4.8%). These consumption patterns are reflected in the natural gas distribution system (Figure 6a) and the predicted  $PM_{0.1}$  concentration field associated with natural gas combustion (Figure 6b). Natural gas end-use included electric power generation (36%), industrial applications (34%), residential use (16%), commercial use (11%), and transportation (3%).

Lane et al. (2007) used a source-resolved version of PMCAMx and individual emission inventories to determine source contributions of primary organic material ( $POM_{2.5}$ ) (Lane, Pinder et al. 2007). Lane et al. note that  $POM_{2.5}$  associated with natural gas sources ranged from 0.1 to  $0.8 \mu\text{g}/\text{m}^3$ . Chang et al in 2004 measured emitted particle size distributions for gas-fired stationary combustion that fell between 10-100nm (Chang, Chow et al. 2004). The combination of these two results indicates that the natural gas mass component of  $POM_{2.5}$  predicted by Lane et al. is consistent with the magnitude of the  $PM_{0.1}$  mass associated with natural gas combustion



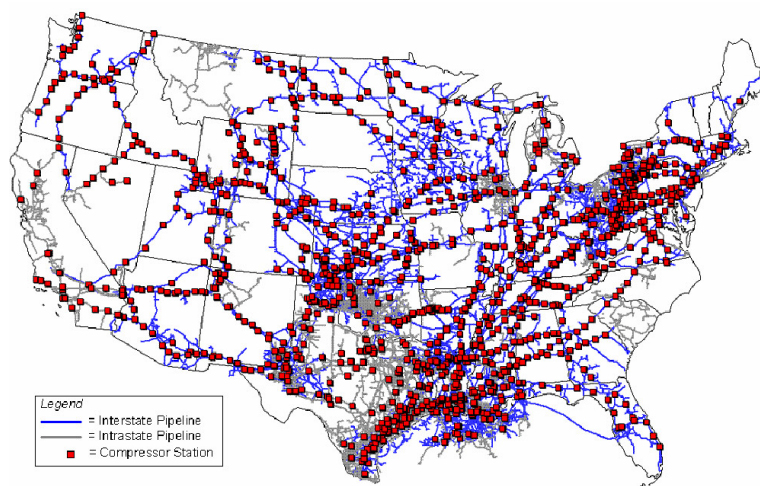
found in the current study. Lane et al. were not studying  $PM_{0.1}$  and so the major role of natural gas in this size fraction was not identified.

Posner and Pandis (2015) utilized PMCAMx with the LADCO 2001 BaseE source-resolved mass emissions inventory for a July 2001 prediction of PNC over the Eastern United States with 36 km resolution (Posner and Pandis 2015). Posner and Pandis used a “zero-out” method in combination with source-specific size distribution to study the percent contribution of six major sources (on road gasoline, industrial, non-road diesel, on road diesel, biomass and dust) of PNC. They found that PNC was made up of 36% on-road gasoline, 31% industrial, 18% non-road diesel, 10% on-road diesel, 1% biomass burning and 4% long-range transport (Posner and Pandis 2015). The emissions particle number inventory was normalized based on  $PM_{10}$  mass from each source and particle emissions from natural gas sources were assumed negligible, which effectively removed natural gas sources from the simulation. This has minor effects on  $PM_{2.5}$  and  $PM_{10}$  predictions, but the results of the current study suggest that natural gas combustion contributes significantly to ultrafine particle concentrations.

355



(a) Natural Gas Compressor Stations and Pipelines throughout the U.S. (Map courtesy of U.S. Energy Information Administration)



(b) UCD/CIT CTM Field Plot of  $PM_{0.1}$  from Natural Gas sources

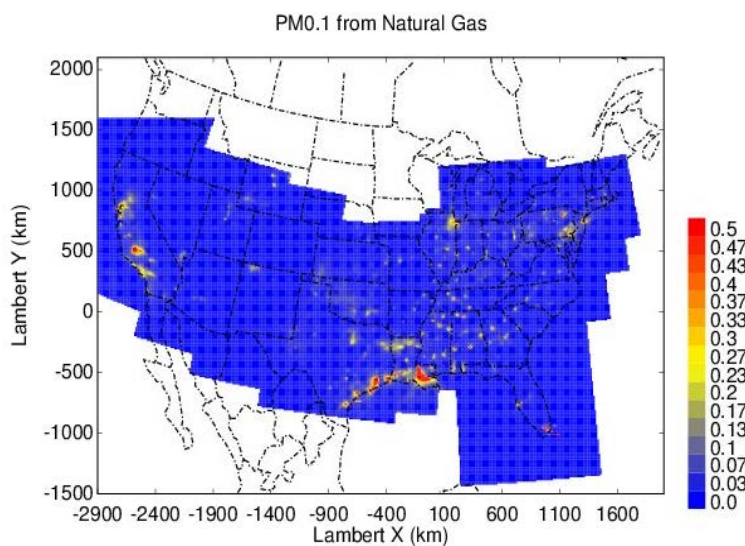


Figure 6. (a) Natural Gas compressor stations and pipelines across the US and (b)  $PM_{0.1}$  Natural Gas combustion concentrations ( $\mu\text{g m}^{-3}$ ).



Future epidemiological studies may be able to differentiate  $PM_{0.1}$  and  $PM_{2.5}$  health effects by contrasting cities with different ratios of  $PM_{0.1}$  /  $PM_{2.5}$ . Figure 7 illustrates the correlation between  $PM_{2.5}$  and  $PM_{0.1}$  concentrations in the 39 cities considered in the current analysis. Cities with higher  $PM_{0.1}$  /  $PM_{2.5}$  ratios include Houston TX, Los Angeles CA, Birmingham AL, Charlotte NC, and Bakersfield CA. Cities with lower  $PM_{0.1}$  to  $PM_{2.5}$  ratios include Lake Charles LA, Baton Rouge LA, St. Louis MO, Baltimore MD, and Washington DC. Measurements should be conducted in these locations to verify the contrast in  $PM_{0.1}$  /  $PM_{2.5}$  concentrations in preparation for future exposure analysis.

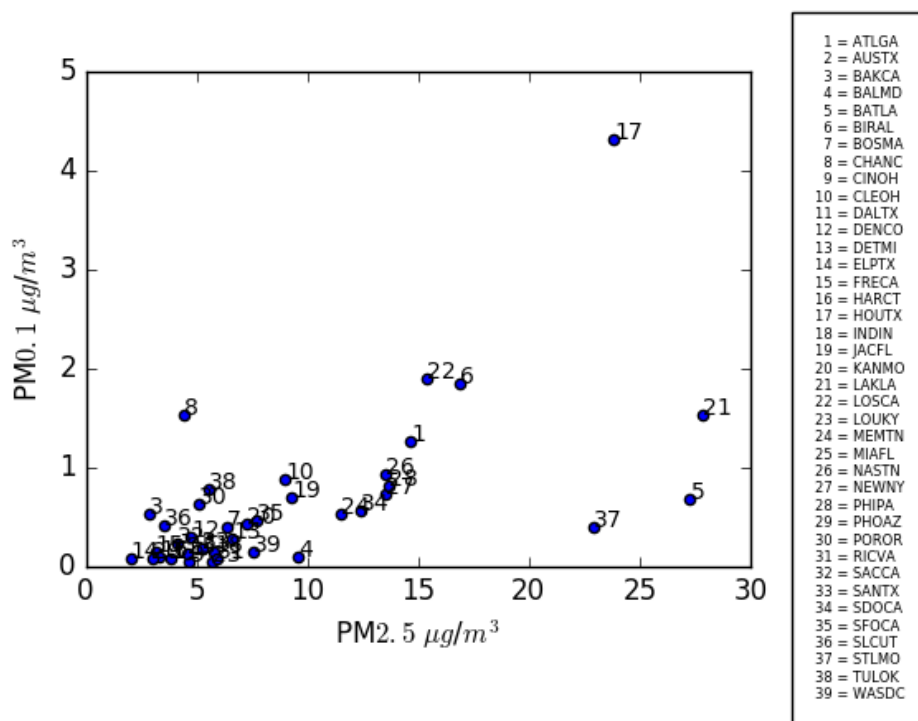


Figure 7. Scatter plot showing correlation between 24-hr average  $PM_{2.5}$  and  $PM_{0.1}$  for the 39-cities.

Future epidemiological studies may also be able to use the contrast in  $PM_{0.1}$  source contributions between different cities to separately identify health effects. In the current study, the similarity in  $PM_{0.1}$  source contributions between cities was calculated as a dot product. A



source contribution vector was created for each city with 13 elements set equal to the normalized % contribution from each source. The dot product of each city source-vector with other city source-vectors was then calculated using eq. (2)

380

$$\vec{a} \cdot \vec{b} = \|\vec{a}\| \|\vec{b}\| \cos(\theta) \quad (2)$$

where  $\vec{a}$  is the vector of city  $i$ ,  $\vec{b}$  is the vector of source for city  $j$ ,  $\|\vec{a}\|$  is the magnitude of city  $i$ ,  $\|\vec{b}\|$  is the magnitude of the vector for city  $j$  and  $\theta$  is the angle between the two vectors ranging from 0 to 90°.  $\cos(\theta)$  quantifies the similarity in source contributions between the two cities. Rearranging Eq. (2)  $\cos(\theta)$  can be solved using Eq. (3)

385

$$\cos(\theta) = \left( \frac{\vec{a} \cdot \vec{b}}{\|\vec{a}\| \|\vec{b}\|} \right) \quad (3)$$

390  $\cos(\theta)$  ranges between zero (0) for no correlation to one (1) for perfect correlation between the source vectors. Figure 8 illustrates the value of  $\cos(\theta)$  calculated for city comparisons for PM<sub>0.1</sub> (lower left) and PM<sub>2.5</sub> (upper right) source-vectors. The cities were arranged by region defined in Table 1 and starting from East, South East, South, Midwest and West in order to observe any geographical patterns. PM<sub>2.5</sub> source-vectors were found to be slightly more homogenous across all U.S. cities than PM<sub>0.1</sub> source vectors. Regional clusters with similar source contributions are apparent, especially on the East Coast where cities are closer in proximity to one another. Few regional clusters were observed for PM<sub>0.1</sub> source vectors, suggesting that emissions control programs may need to be tailored to each region. Natural gas combustion is prevalent in many locations, but the remaining sources of ultrafine particles vary strongly with location.

400

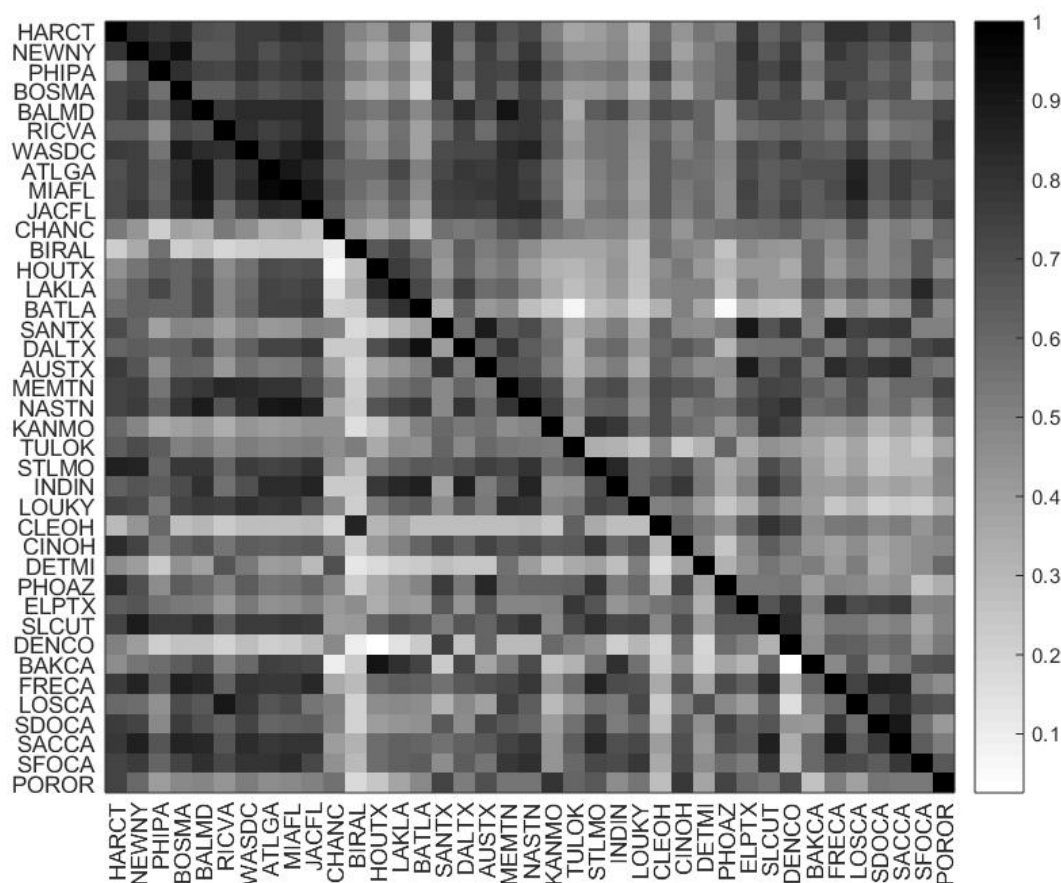


Figure 8. Normalized dot product between the 13 source types and each city for PM<sub>2.5</sub> (upper right) and PM<sub>0.1</sub> (lower left). The scale represents 100% (black) to 0% (white) correlation. Cities are organized by region in the following order: East, South East, South, Midwest and West.

## 5. Conclusion

The UCD/CIT regional chemical transport model was used to predict source contributions to PM<sub>0.1</sub> across the continental United States during peak photochemical smog periods during the year 2010. Model performance for PM<sub>2.5</sub> and ozone predictions met the recommendations for regulatory applications building confidence in the emissions inputs and meteorological fields used to drive the calculations. Similar model exercises carried out for episodes in California in 2015 and 2016 find good agreement between predicted PM<sub>0.1</sub> source



415 contributions and receptor-based  $PM_{0.1}$  source contributions calculated using measured  
concentrations of molecular markers (Yu, Venecek et al. 2018). Regional  $PM_{0.1}$  concentrations  
exceeded  $2 \mu g m^{-3}$  during summer pollution episodes in major urban regions across the US  
including Los Angeles, the San Francisco Bay Area, Houston, Miami, and New York.  $PM_{0.1}$   
spatial gradients were sharper than  $PM_{2.5}$  spatial gradients due to the dominance of primary  
420 aerosol in  $PM_{0.1}$ . This finding suggests that  $PM_{0.1}$  measurement networks needed to support  
epidemiology must be denser than comparable  $PM_{2.5}$  measurement networks. Non-residential  
natural gas combustion was identified as a major source of  $PM_{0.1}$  across all major cities in the  
United States. On-road gasoline and diesel vehicles made significant contributions to regional  
 $PM_{0.1}$  in all 39 cities even though peak contributions within 0.3 km of the roadway were not  
425 resolved by the 4 km grid cells. This is consistent with other studies that have found an  
exponential decrease in ultrafine particle concentrations outside of major roadways (Wang,  
Hopke et al. 2011). Food cooking also made significant contributions to  $PM_{0.1}$  in all cities but  
biomass combustion was only important in locations impacted by summer wildfires. Aviation  
was a significant source of  $PM_{0.1}$  in cities that had airports within their urban footprints. The  
430 major sources of primary  $PM_{0.1}$  and  $PM_{2.5}$  were notably different in many cities. Future  
epidemiological studies may be able to differentiate  $PM_{0.1}$  and  $PM_{2.5}$  health effects by contrasting  
cities with different ratios of  $PM_{0.1} / PM_{2.5}$  sources.

**Data Availability:** All of the  $PM_{0.1}$  and PNC outdoor exposure fields produced in the current  
435 study are available free of charge at <http://faculty.engineering.ucdavis.edu/kleeman/>.

**Acknowledgements:** This research was supported by the California Air Resources Board under  
project #14-314. Neither CARB nor any person acting on their behalf: (1) makes any warranty,  
express or implied, with respect to the use of any information, apparatus, method, or process  
440 disclosed in this report, or (2) assumes any liabilities with respect to use, or damages resulting  
from the use or inability to use, any information, apparatus, method, or process disclosed in this  
report.





## References

- 445 Aneja, A. P., P. R. Pillai, A. Isherwood, P. Morgan and S. P. Aneja (2017). "Particulate matter pollution in the coal-producing regions of the Appalachian Mountains: Integrated ground-based measurements and satellite analysis." *Journal of Air and Waste Management Association* **67**(4): 421-430.
- Baxter, L. K., R. M. Duvall and J. Sacks (2013). "Examining the effects of air pollution composition on within region differences in PM<sub>2.5</sub> mortality risk estimates." *J Expo Sci Environ Epidemiol* **23**(5): 457-465.
- 450 Bergin, M. S., A. G. Russell, Y. J. Yang, J. B. Milford, F. Kirchner and W. R. Stockwell (1996). "Effects of uncertainty in SAPRC90 rate constants and selected product yields on reactivity adjustment factors for alternative fuel vehicle emissions. Final Report."
- Cappa, C. D., S. H. Jathar, M. J. Kleeman, K. S. Docherty, J. L. Jimenez, J. H. Seinfeld and A. S. Wexler (2016). "Simulating secondary organic aerosol in a regional air quality model using the statistical oxidation model - Part 2: assessing the influence of vapor wall losses." *Atmos. Chem. Phys.* **16**: 3041-3059.
- 455 Carlton, A. G., P. V. Bhawe, S. L. Napelenok, E. D. Edney, G. Sarwa, R. W. Pinder, G. A. Pouliot and M. Houyoux (2010). "Model representation of secondary organic aerosol in CMAQv4.7." *Environmental Science and Technology* **44**: 8553-8560.
- 460 Carter, W. P. L. and G. Heo (2013). "Development of Revised SAPRC Aromatics Mechanisms." *Atmospheric Environment* **77**: 404-414.
- Cattani, G., A. Gaeta, A. Di Menno di Bucchianico, A. De Santis, R. Gaddi, M. Cusano, C. Ancona, C. Badaloni, F. Forastiere, C. Gariazzo, R. Sozzi, M. Inglessis, C. Silibello, E. Salvatori, F. Manes and G. Cesaroni (2017). "Development of land-use regression models for exposure assessment to ultrafine particles in Rome, Italy." *Atmospheric Environment* **156**: 52-60.
- 465 Chang, M.-C., J. C. Chow, J. G. Watson, P. K. Hopke, S.-M. Yi and G. C. England (2004). "Measurement of Ultrafine Particle Size Distributions from Coal-, Oil-, and Gas-Fired Stationary Combustion Sources." *Journal of Air and Waste Management Association* **54**(12): 1494-1505.
- 470 Dominici, F., R. D. Peng, M. L. Bell, L. Pham, A. McDermott, S. L. Zeger and J. Samet, M. (2006). "Fine Particulate Air Pollution and Hospital Admission for Cardiovascular and Respiratory Diseases." *JAMA* **295**(10): 1127-1134.
- Energy, U. S. D. o. (2017). "Natural Gas Explained, Use of Natural Gas." from [https://www.eia.gov/energyexplained/index.php?page=natural\\_gas\\_use](https://www.eia.gov/energyexplained/index.php?page=natural_gas_use).
- 475 EPA, U. "AQS API / Query AirData." from [aqds.epa.gov/api](https://aqds.epa.gov/api).
- EPA, U. (2017). "Air Quality Designations for Particle Pollution." from <https://www.epa.gov/pm-pollution/forms/contact-us-about-particulate-matter-pm-pollution>.
- Franklin, M., A. Zeka and J. Schwartz (2007). "Association between PM<sub>2.5</sub> and all-cause and specific-cause mortality in 27 US communities." *Journal of Exposure Science and Environmental Epidemiology* **17**: 279-287.
- 480 Gaydos, T. M., C. O. Stanier and S. N. Pandis (2005). "Modeling of in situ ultrafine atmospheric particle formation in the eastern United States." *Journal of Geophysical Research* **110**.
- Giglio, L., J. T. Randerson and G. R. van der Werf (2013). "Analysis of daily, monthly and annual burned area using the fourth-generation global fire emissions database (GFED4)." *Journal of Geophysical Research* **118**(1): 317-328.
- 485 Guenther, A. B., X. Jiang, C. L. Heald, T. Sakulyanontvittaya, T. Duhl, K. Emmons and X. Wang (2012). "The Model of Emissions of Gases and Aerosols from Nature version 2.1 (MEGAN2.1): an extended and updated framework modeling biogenic emissions." *Geoscientific Model Development* **5**: 1471-1492.
- Ham, W. A. and M. J. Kleeman (2011). "Size-resolved source apportionment of carbonaceous particulate matter in urban and rural sites in central California." *Atmospheric Environment* **45**: 3988-3995.
- 490





- Held, T., Q. Ying, M. Kleeman, J. Schauer and M. Fraser (2005). "A comparison of the UCD/CIT air quality model and the CMB source-receptor model for primary airborne particulate matter." Atmospheric Environment **39**: 2281-2297.
- 495 Hu, J., H. Zhang, S. Chen, C. Wiedinmyer, F. Vanderbergh, Q. Ying and M. J. Kleeman (2014). "Predicting Primary PM<sub>2.5</sub> and PM<sub>0.1</sub> Trace Composition for Epidemiological Studies in California" Environmental Science and Technology **48**(9): 4971-4979.
- Hu, X.-M., Y. Zhang, M. Z. Jacobson and C. K. Chan (2008). "Coupling and evaluating gas/particle mass transfer treatments for aerosol simulation and forecast." J. Geophys. Res. **113**(D11208).
- 500 Kheirbek, I., K. Wheeler, S. Walters, D. Kass and T. Matte (2013). "PM<sub>2.5</sub> and Ozone health impacts and disparities in New York City: sensitivity to spatial and temporal resolution." Air Qual Atmos Health **6**: 473-486.
- Kleeman, M. J., S. G. Riddle, M. A. Robert, C. A. Jakober, P. M. Fine, M. D. Hays, J. J. Schauer and M. P. Hannigan (2009). "Source Apportionment of Fine (PM<sub>1.8</sub>) and Ultrafine (PM<sub>0.1</sub>) Airborne Particulate Matter during a Severe Winter Pollution Episode." Environmental Science and Technology **43**(2): 272-279.
- 505 Kleeman, M. J., M. A. Robert, S. G. Riddle, P. M. Fine, M. D. Hays, J. J. Schauer and M. P. Hannigan (2008). "Size distribution of trace organic species emitted from biomass combustion and meat charbroiling." Atmos. Environ. **42**(24): 3059.
- Laden, F., L. M. Neas, D. W. Dockert and J. Schwartz (2000). "Association of fine particulate matter from different sources with daily mortality in six U.S. Cities." Environ Health Persp. **108**(10): 941-947.
- 510 Lane, T. E., R. W. Pinder, M. Shrivastava, A. L. Robinson and S. N. Pandis (2007). "Source contributions to primary organic aerosol: Comparison of the results of a source-resolved model and the chemical mass balance approach." Atmospheric Environment **41**: 3758-3776.
- Laurent, O., J. Hu, L. Li, M. J. Kleeman, S. M. Bartell, M. Cockburn, L. Escobedo and J. Wu (2016). "A Statewide Nested Case-Control Study of Preterm Birth and Air Pollution by Source and Composition: California, 2001-2008." Environmental Health Perspectives.
- 515 Li, N., C. Siotas, A. Cho, D. Schmitz, C. Misra, S. J., M. Y. Wang, T. Oberley, J. Froines and A. Nel (2003). "Ultrafine particulate pollutants induce oxidative stress and mitochondrial damage." Environ Health Persp. **111**(4): 455-460.
- 520 Nel, A., T. Xia, L. Madler and N. Li (2006). "Toxic potential of materials at the nanolevel" Science **311**(5761): 622-627.
- Nenes, A., C. Pilinis and S. N. Pandis (1998). "ISORROPIA: A new thermodynamic equilibrium model for multiphase multicomponent marine aerosols" Aquat. Geochem **4**: 123-152.
- 525 Oberdorster, G., R. Gelein, J. Ferin and B. Weiss (1995). "Association of Particulate Air Pollution and ACute Mortality: Involvement of Ultrafine Particles." Inhal. Toxicol. **7**: 111-124.
- Oberdorster, G. (2000). "Toxicology of ultrafine particles: in vivo studies." The Royal Society **358**(1175).
- Ostro, B., R. Broadwin, S. Green, W. Y. Feng and M. Lipsett (2006). "Fine particulate air pollution and mortality in nine California counties: Results from CALFINE." Environ Health Persp. **114**(1): 29-33.
- 530 Ostro, B., J. Hu, D. Goldber, P. Reynolds, A. Hertz, L. Bernstein and M. J. Kleeman (2015). "Associations of mortality with long-term exposures to fine and ultrafine particles, species and sources: results from the California Teachers Study Cohort." Environ Health Persp. **123**(6): 549-556.
- Pekkanen, J., K. L. Timonen, J. Ruuskanen, A. Reponen and A. Mirme (1997). "Effects of Ultra-Fine and fine PArticles in Urban Air on Peak Expiratory Flow Among Children with Asthmatic Symptoms." Environ. Res. **74**: 24-33.
- 535 Pope, C. A., R. T. Burnett, M. J. Thun, E. E. Calle, D. Krewski, K. Ito and G. D. Thursdton (2002). "Lung Cancer, Cardiopulmonary Mortality and Long Term Exposure to Fine Particulate Air Pollution." JAMA-J AM Med Assoc. **287**(8): 1132-1141.



- Pope, C. A., M. Ezzati and D. W. Dockery (2009). "Fine-Particulate Air Pollution and US County Life Expectancies." New Engl J Med. **360**(4): 376-386.
- 540 Posner, L. A. and S. N. Pandis (2015). "Sources of ultrafine particles in the Eastern United States." Atmospheric Environment **111**: 103-112.
- Reff, A., P. V. Bhawe, H. Simon, T. G. Pace, G. A. Pouliot, J. D. Mobley and M. Houyoux (2009). "Emissions Inventory of PM<sub>2.5</sub> TRace Elements across the United States." Environmental Science and Technology **43**(15): 5790-5796.
- 545 Robert, M. A., M. J. Kleeman and C. A. Jakober (2007b). "Size and composition distributions of particulate matter emissions: Part 2 - Heavy - duty diesel vehicles." J. Air Waste Management **57**(12): 1429-1438.
- Robert, M. A., S. VanBergen, M. J. Kleeman and C. A. Jakober (2007a). "Size and Composition distributions of particulate matter emissions: Part 1 - Light duty gasoline vehicles." J. Air Waste Management **57**(12): 1414-1428.
- 550 Simon, M. C., A. P. Patton, E. N. Naumova, J. I. Levy, P. Kumar, D. Brugge and J. L. Durant (2018). "Combining Measurements from Mobile Monitoring and a Reference Site to Develop Models of Ambient Ultrafine Particle Number Concentrations at Residences." Environ. Sci. Technol **52**(12): 6985-6995.
- Sioutas, C., R. J. Delfino and M. Singh (2005). "Exposure assessment for atmospheric ultrafine particles (UFPs) and implications in epidemiologic research." Environ Health Persp. **113**(8): 947-955.
- 555 Solomon, P. A., D. Crumpler, J. B. Flanagan, R. K. M. Jayant, E. E. Rickman and C. E. McDade (2014). "U.S. National PM<sub>2.5</sub> Chemical Speciation Monitoring Networks - CSN and IMPROVE: Description of networks." Journal of Air and Waste Management Association **64**(12): 1410-1438.
- Wang, Y., P. K. Hopke, D. C. Chalupa and M. J. Utell (2011). "Long-term study of urban ultrafine particles and other pollutants." Atmospheric Environment **45**: 7672-7680.
- 560 Wolf, K., J. Cyrys, T. Hacinikova, J. Gu, T. Kusch, R. Hampel, A. Schneider and A. Peters (2017). "Land use regression modeling of ultrafine particles, ozone, nitrogen oxides and markers of particulate matter pollution in Augsburg, Germany." Science of the Total Environment **579**: 1531-1540.
- Xue, J., W. Xue, M. Sowlat, C. Sioutas, A. Lilioco, A. Hasson and M. Kleeman (2018). "Annual trends in ultrafine particulate matter (PM<sub>0.1</sub>) source contributions in polluted California cities." Environmental Science and Technology **in review**.
- 565 Yu, X., M. Venecek, J. Hu, S. Tanrikulu, S.-T. Soon, T. Cuong, D. Fairley and M. J. Kleeman (2018). "Regional Ultrafine Particle Number and Mass Concentrations in California." Atmos. Chem. Phys **submitted for publication**.
- Zhang, H., J. Hu, M. Kleeman and Q. Ying (2014). "Source apportionment of sulfate and nitrate particulate matter in the Eastern United States and Effectiveness of emission control programs." Science of the Total Environment **490**: 171-181.
- 570 Zheng, M., G. R. Cass, J. J. Schauer and E. S. Edgerton (2002). "Source Apportionment of PM<sub>2.5</sub> in the Southeastern United States Using Solvent-Extractable Organic Compounds as Tracers." Environmental Science and Technology **36**(11): 2361-2371.
- 575 Zhong, J., I. Nikolova, X. Cai, A. R. MacKenzie and R. M. Harrison (2018). "Modelling traffic-induced multicomponent ultrafine particles in urban street canyon compartments: Factors that inhibit mixing." Environmental Pollution **238**: 186-195.